# Quasi-Two-Dimensional Electrodeposition under Forced Fluid Flow

Laura López-Tomàs, Josep Claret, and Francesc Sagués
*Departament de Química-Física, Universitat de Barcelona, Martí i Franquès 1, 08028 Barcelona, Spain*
(Received 3 February 1993; revised manuscript received 30 July 1993)

Experimental quasi-two-dimensional Zn electrodeposits are grown under forced convection conditions. Large-scale effects, with preferential growth towards the impinging flow, together with small-scale roughness suppression effects are evidenced and separately analyzed by using two different radial cell configurations. Interpretations are given in terms of primary concepts concerning current and concentration distributions.

PACS numbers: 68.70.+w, 47.32.−y, 82.45.+z

The intriguing complexity of patterns grown under nonequilibrium conditions [1] cannot be understood without appropriately considering the distinct length scales, and associated controlling fields, involved during growth. This is particularly true in electrochemical deposition (ECD) where the elucidation of the specific roles of the electric (Laplacian) and concentration (diffusion) fields has recently been the subject of close scrutiny [2–6]. The picture which is emerging from this intensive research is that apart from crystallization effects conforming the micron-size crystallites of the aggregate, gross features, such as those associated with the deposit growing front, typical of the electric field length scale, i.e., the cell size, coexist with the smaller length scale details of the branched texture developed inside the concentration boundary layer which encompass the metallic interface. In this Letter this question is addressed from a different and completely original perspective by reporting on experiments of quasi-two-dimensional ECD with imposed bulk flow. Coupled differently to the Laplacian and diffusion fields, convection flow provides us with new experimental conditions to check the precedent view of the standard ECD growth mechanism. Although various authors [7,8] have recently examined the possible role played by natural convection in ECD, previous studies of ECD under controlled flow conditions are very scarce [9]. In the related context of crystal growth, thermal and forced convection effects have been reported by Gill [10].

Using appropriately chosen configurations of the two-electrode system, we evidence distinctive length scale dependent effects of superimposed bulk flow on the morphology of the electrodeposits. On a cell length scale and due to the large values of the Prandtl (or Schmidt) number typical of our experimental conditions ($P_r = \nu/D \approx 10^3$; $\nu$, kinematic viscosity; $D$, diffusion coefficient), purely convective transport (advection) couples with ionic migration to largely modify the Laplacian primary distribution, and, correspondingly, the observed preferred growth directions of the metallic deposit. In addition, roughness suppression on the much smaller diffusion length scales is evidenced and explained in terms of a directed flow-induced shrinking of the concentration boundary layer. Interpreted distinctively under such general principles, our results are expected to have wider implications for pattern formation generally, either single field induced (Laplacian or diffusion) [1], or for other two-field systems such as directional solidification [11] and amorphous annealing [12].

Our experimental cell is similar to those employed in Refs. [13] and [14]. It consists of a Petri dish, typically 12 cm in diameter, with an aqueous-organic interface separating the ionic solution, here $ZnSO_4$ (aq), from an upper phase of *n*-butyl acetate. Analytical reagent-grade chemicals were used in all the experiments, and temperature control was achieved by using a thermostating jacket around the Petri dish. Preliminary experiments led us to fix the most convenient growth conditions as those corresponding to a $2M$ $ZnSO_4$ solution electrolyzed at 15 °C. Images of the growing deposit were taken with both a photo and a video camera and digitized when necessary to a resolution of 512×512 pixels. For enlarged views a stereo-zoom microscope Olympus SZH was employed. The Petri dish was placed on a rotating plate which provided us with the well-controlled convective motion of the liquid phases relative to the fixed rodlike shaped electrodes. The cathode was a cylindrical graphite bar, 0.5 mm in diameter, and the anode was composed of metallic Zn (99.99%) with a squared cross section of 2 mm on a side. Both were carefully positioned at the interface with a micromanipulator in order to assure the closest conditions to a two-dimensional growth. In the last experiments here reported a Cu deposit was grown in a surfactant (Triton-X) stabilized thin film of a $0.5M$ $CuSO_4$ solution (5 ml) with a Cu wire (99.99%) anode. To render it colored a small amount of a dark anion $NBB^{-2}$ (naphtol blue-black) was added: 4 ml of CuNBB (ca. $4.5\times10^{-3}M$).

Experiments employing a ring-shaped Zn anode disposed along the internal perimeter of the Petri cell which had centrally placed the graphite cathode had been preliminarily conducted and have been reported in a recent paper [15]. Convective effects, expected there to be stronger as the deposit grew, appeared sometimes masked by those purely originated by the approached anode. In contrast, the use of pointlike electrodes, offers, as it will become clear below, the opportunity to choose the cell

0031-9007/93/71(26)/4373(4)$06.00

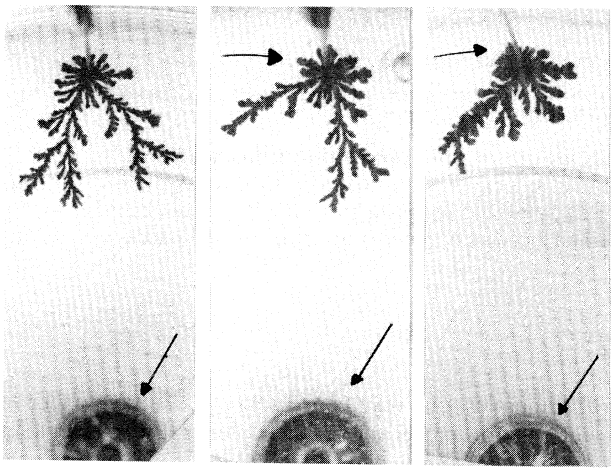

(a) (b) (c)

FIG. 1. Zinc electrodeposits grown with the forced fluid flow, acting as indicated by the upper arrow, on a quasiperpendicular direction with respect to the applied electric field. Values of rotation rate are (a) 0 rpm, (b) 6 rpm, and (c) 12 rpm. $\Delta V = 10$ V for all the flow conditions. The lower arrow shows the place of the anode.

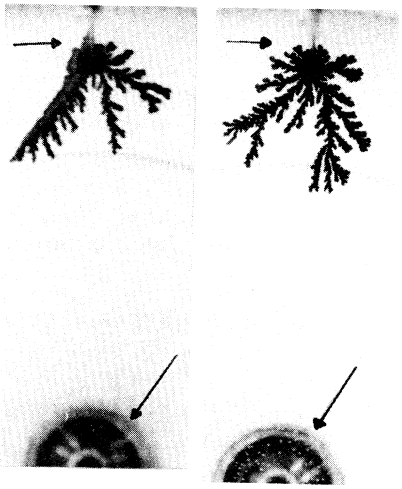

(a) (b)

FIG. 2. Zinc electrodeposits grown under the maximum fluid flow intensity (12 rpm). To compare with Fig. 1(c), conditions here correspond to (a) $\Delta V = 15$ V and (b) $\Delta V = 20$ V.

configuration most appropriate to the investigated convection effect. Actually, two different electrode locations were analyzed, which differed in the relative orientation of the hydrodynamic and electric fields. In the first one, hereafter referred to as the quasiperpendicular configuration, the anode is placed at the center of the Petri dish cell and the cathode is radially separated 5 cm apart from it. The second selected complementary configuration, referred to here as quasiparallel, consisted of two electrodes kept equidistant 5 cm apart from the center of the cell with a fixed angular separation of 60° (upstream anode). In both situations, a series of experiments was conducted varying the applied potential and rotation speed: $\Delta V = 5$–$20$ V; $\omega = 0$–$12$ rpm.

*Quasiperpendicular configuration.*—Typical patterns grown under this configuration are shown in Fig. 1. They correspond to different intensities of the fluid flow, while keeping constant the applied potential difference. The gross morphological change observed in the pictures is appropriately described in terms of the marked asymmetry acquired by the metallic deposits grown under bulk flow conditions. Actually the resulting pattern is shaped according to what seems to be a competition between the electric and fluid flow fields. As the convection strength increases from 1(a) to 1(c) the radial, essentially migration mediated, growth mode appears progressively balanced by the tangential, bulk flow contribution. This finally results in a metallic aggregate which, while preserving its branched texture, is mostly concentrated along a direction inclined towards the impinging flow. The confirmation that what we are really facing is a balance between the migration and convective forces is even better exhibited in Fig. 2, where $\Delta V$ is varied while keeping constant $\omega$ at its maximum investigated value. Again in this case the aggregate grown under progressively higher electric field strengths is forced to recover its convection-free radially symmetric orientation.

Although the growth of the deposit sensibly alters the initially simple distribution of the coupled migration-diffusion-convection fields, and hence prevents our pursuing any realistic analytical treatment of such growth conditions, the behavior just described may be qualitatively interpreted according to both classical solutions of flow-modified primary (Laplacian) current distributions [16] and recent computer simulations [15,17]. According to both approaches, a prominent upstream anisotropy of the Laplacian field distribution is predicted. In our particular geometry, this would favor deposition on the semicircular cathodic perimeter facing the impinging flow, preferably from the inner quadrant closest to the cathode.

The large-scale morphological effect just mentioned is by no means the unique distinctive feature of the patterns shown in Figs. 1 and 2 resulting from the convection conditions here investigated. A closer view of the patterns (Fig. 3) focusing on the lateral ramification of the inclined metallic branch growing under strong flow strengths reveals that the side facing the impinging flow appears to be remarkably more stable against the development of secondary protrusions than that opposite to it. This sort of branching suppression mechanism, which in principle could be naively attributed to a pure screening effect of the current lines laying from the central anode, is better analyzed and, as explained below more properly interpreted, by referring to the quasiparallel electrode configuration.

*Quasiparallel configuration.*—Typical small-scale pat-

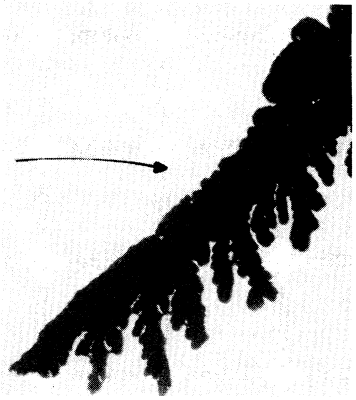

FIG. 3. Enlarged view of the main branch of a zinc electrodeposit for conditions in Fig. 2(a).

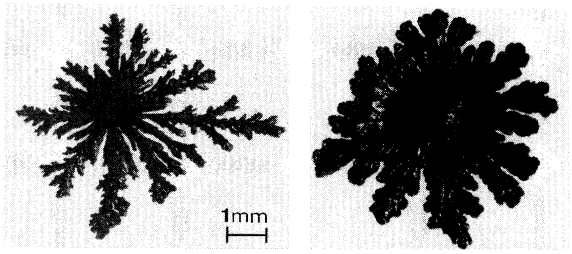


FIG. 4. Small-scale images of the initial development of zinc electrodeposits grown with the forced fluid flow applied quasiparallel to the imposed electric field. The growth area directly exposed to the fluid flow corresponds to the south hemisphere of the presented images. Conditions are as in Fig. 1 for (a) 0 rpm and (b) 12 rpm.

terns grown with this electrode arrangement are shown in Fig. 4. The pictures are taken here at a very early stage of the deposit growth, just after the interfacial instability destroys the inner circular metallic core. The clear conclusion is that roughness is indeed largely suppressed by the impinging flow. A convenient quantitative evaluation of this effect is introduced through the standard roughness $\sigma$ which is a measure of the active zone width [18]: $\sigma=[(N-1)^{-1}\sum_i(R_i-R)^2]^{1/2}$; $R=N^{-1}\sum_i R_i$, where $R_i$ stands for the radius relative to the central cathode of each of the $N$ set surface sites. In Fig. 5 representative plots of the relative quantity $\sigma_R\equiv\sigma/R$ are shown for different values of $\Delta V$ and $\omega$. Roughness suppression is clearly exhibited when increasing the strength of the convective flow. However, even more important is the remarkable effect of the applied potential. Roughness suppression by impinging flow appears to be an extremely effective mechanism under low applied potentials, paradigmatically represented by conditions with $\Delta V=5$ or 10 V. However, under larger electric fields, fluid flow effects do not seem to be capable of so drastically decreasing the inherent branching instability of the exposed surface. In this respect the experiments with $\Delta V=20$ V are especially significant since they display hardly any relevant effects of roughness suppression.

The small-scale, roughness suppression, effects we are describing admit a clear interpretation by considering the compression effect of the directed flow on the impinged concentration boundary layer surrounding the branched interface, since, following the general principle of diffusion mediated small-scale instabilities [19], only irregularities of size $l\leq l_{\rm dif}$ are diffusively supported. This argument is further corroborated by direct experimental observations, shown in Fig. 6, and by a simple scaling argument plotted in the inset of Fig. 5. The concentration boundary layer is imaged in Fig. 6. Specifically, the two pictures correspond to growth in the quasiparallel configuration using the copper solution. The depleted colorless concentration boundary layer of $Cu^{2+}$ cations, and correspondingly of $NBB^{-2}$ anions, appears homogeneously surrounding the whole metallic interface in the absence of bulk flow [Fig. 6(a)]. In marked contrast, Fig. 6(b) (3 rpm) displays a practically unobservable concentration layer on the upstream smooth side, while it clearly appears and extends from the much more irregular down-

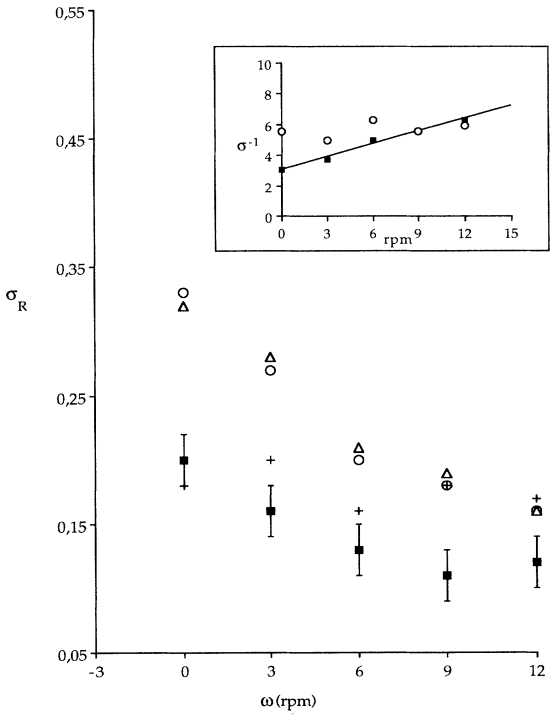


FIG. 5. Roughness of the growing interface directly exposed to the impinging flow, plotted against flow intensities for different electric field strengths. ○: 5 V; △: 10 V; ■: 15 V; +: 20 V. Typical error bars are shown. In the inset, the scaling $\sigma_R^{-1}\propto 1+a|v_f|$ is depicted for 5 V (■) and 20 V (○). For the first set of points a linear fit is proposed ($R^2=0.98$).

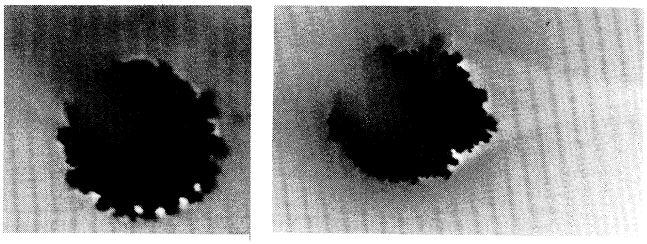

(a) (b)

FIG. 6. Images of electrodeposition of copper evidencing the concentration boundary layer. Flow conditions are (a) 0 rpm and (b) 3 rpm. The size of the deposits is about 1 mm.

stream side of the growing deposit. Analytically, the nonrigorous argument that predicts a compression of the effective diffusion length by an impinging flow ($v_f$) superimposed to the normal operation of a diffusion field is formulated quite simply from the diffusion-convection equation [20]. The growth is assumed to follow the positive $z$ direction, so that the quasi-steady-state approximation transforms such an equation into

$$D\frac{\partial^2 C}{\partial z^2}+(v_g-v_f)\frac{\partial C}{\partial z}=0,$$

with $v_f<0$ and $v_g>0$ for the growth velocity. Thus, $l_{\text{dif}} \sim D(v_g-v_f)^{-1}$, and taking $\sigma_R$ as a measure of $l_{\text{dif}}$, we end up with $\sigma_R^{-1}\propto 1+a|v_f|$. Such a scaling is recovered, as depicted in the inset of Fig. 5, for the conditions of maximum roughness suppression, i.e., $\Delta V=5$ V. Not surprisingly it does not apply to the conditions of $\Delta V=20$ V.

In summary, quasi-two-dimensional ECD under bulk flow has been experimentally investigated. Effects on both the gross growth symmetries and finer branched texture have been evidenced. Interpreted distinctively under general principles for both Laplacian and diffusion fields, our results may have implications for other pattern forming systems. In particular, convection demonstrates the influence of the boundary layer on the deposit roughness by suppressing features of a particular size range in a nonsymmetric manner.

Thanks are due to P. P. Trigueros for helpful assistance, and to Centre de Supercomputació de Catalunya, CESCA, for providing the computer time. Financial support from Dirección General de Investigacion Científica y Técnica (Spain) (Project No. PB90-0455) is also acknowledged.

[1] J. S. Langer, Science **243**, 1150 (1989); E. Ben-Jacob and P. Garik, Nature (London) **343**, 523 (1990).
[2] P. Garik, D. Barkey, E. Ben-Jacob, E. Bochner, N. Broxholm, B. Miller, B. Orr, and R. Zamir, Phys. Rev. Lett. **62**, 2703 (1989).
[3] J.-N. Chazalviel, Phys. Rev. A **42**, 7355 (1990); V. Fleury, M. Rosso, J.-N. Chazalviel, and B. Sapoval, Phys. Rev. A **44**, 6693 (1991).
[4] J. R. Melrose, D. B. Hibbert, and R. C. Ball, Phys. Rev. Lett. **65**, 3009 (1990).
[5] D. Barkey, J. Electrochem. Soc. **138**, 2912 (1991); D. Barkey, P. Garik, E. Ben-Jacob, B. Miller, and B. Orr, *ibid.* **139**, 1044 (1992).
[6] F. Mas and F. Sagués, Europhys. Lett. **17**, 541 (1992); J. Mach, F. Mas, and F. Sagués (to be published).
[7] P. Garik, J. Hetrick, B. Orr, D. Barkey, and E. Ben-Jacob, Phys. Rev. Lett. **66**, 1606 (1991).
[8] V. Fleury, J. N. Chazalviel, and M. Rosso, Phys. Rev. Lett. **68**, 2492 (1992).
[9] Using experimental designs more conventional in an electrochemical context, we should cite the works by M. M. Jaksic and V. P. Komnenic, J. Electroanal. Chem. **328**, 127 (1992); J. Jorné, Y. Lii, and K. E. Yee, J. Electrochem. Soc. **134**, 1399 (1987).
[10] W. N. Gill, Chem. Eng. Prog. **85**, 33 (1989).
[11] J. Langer, Rev. Mod. Phys. **52**, 1 (1980), and references therein.
[12] G. Deutscher and Y. Lereah, Phys. Rev. Lett. **60**, 1510 (1988); S. Alexander, R. Bruinsma, R. Helfer, G. Deutscher, and Y. Lereach, *ibid.* **60**, 1514 (1988).
[13] R. Tamamushi and H. Kaneko, Electrochim. Acta **25**, 391 (1980).
[14] M. Matsushita, M. Sano, Y. Hayakawa, H. Honjo, and Y. Sawada, Phys. Rev. Lett. **53**, 286 (1984).
[15] L. López-Tomàs, J. Claret, F. Mas, and F. Sagués, Phys. Rev. B **46**, 11 495 (1992).
[16] J. S. Newman, *Electrochemical Systems* (Prentice Hall, Englewood Cliffs, NJ, 1991), 2nd ed.
[17] R. F. Xiao, J. I. D. Alexander, and F. Rosenberg, Phys. Rev. A **39**, 6397 (1989); T. Nagatani and F. Sagués, *ibid.* **43**, 2970 (1991); S. Seki, M. Uwaha, and Y. Saito, Europhys. Lett. **14**, 397 (1991); J. C. Toussaint, J. M. Debierre, and L. Turban, Phys. Rev. Lett. **68**, 2027 (1992).
[18] F. Family and T. Vicsek, J. Phys. A **18**, L75 (1985).
[19] L. M. Sander, in *The Physics of the Structure Formation*, edited by W. Güttinger and G. Dangelmayr (Springer-Verlag, Berlin, 1987); electrochemical formulations of this principle may be found in the contribution by O. Kardos and D. G. Foulke, in *Advances in Electrochemistry and Electrochemical Engineering*, edited by C. W. Tobias (Interscience Publishers, New York, 1962), Vol. 2; more specialized discussions are those by D. Barkey, R. H. Muller, and C. W. Tobias, J. Electrochem. Soc. **136**, 2199 (1989); **136**, 2207 (1989).
[20] In the context of aggregation from a finite-density lattice gas this argument has also been proposed in the paper by Seki, Uwaha, and Saito (Ref. [17]).

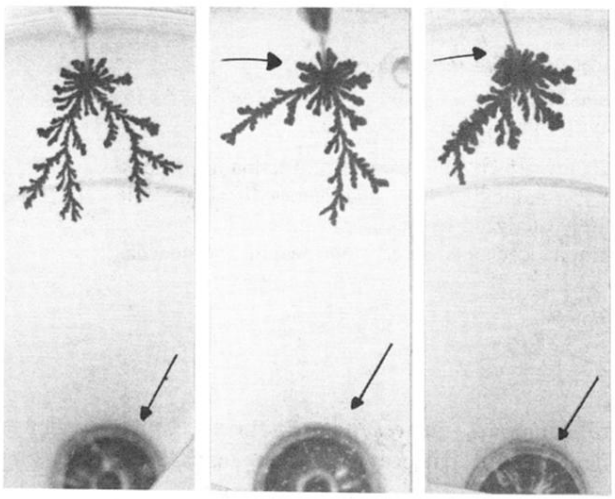

(a) (b) (c)

FIG. 1. Zinc electrodeposits grown with the forced fluid flow, acting as indicated by the upper arrow, on a quasiperpendicular direction with respect to the applied electric field. Values of rotation rate are (a) 0 rpm, (b) 6 rpm, and (c) 12 rpm. $\Delta V = 10$ V for all the flow conditions. The lower arrow shows the place of the anode.

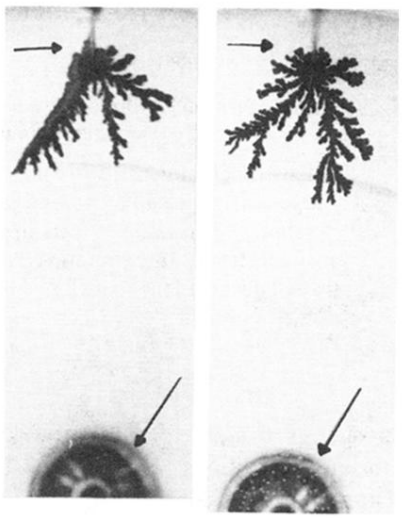

(a) (b)

FIG. 2. Zinc electrodeposits grown under the maximum fluid flow intensity (12 rpm). To compare with Fig. 1(c), conditions here correspond to (a) $\Delta V = 15$ V and (b) $\Delta V = 20$ V.

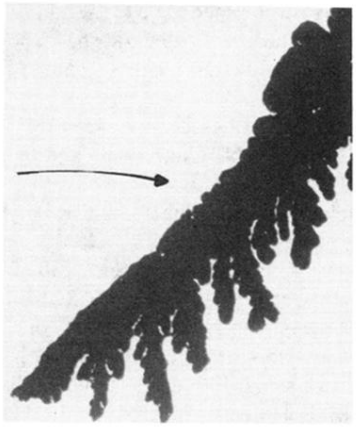

FIG. 3. Enlarged view of the main branch of a zinc electrodeposit for conditions in Fig. 2(a).

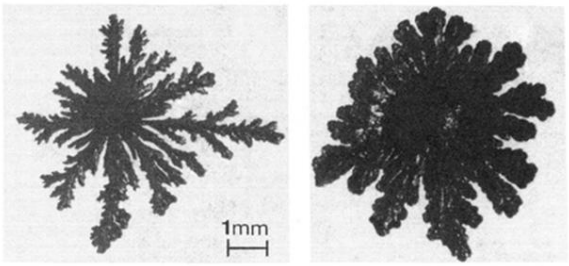


(a) (b)

FIG. 4. Small-scale images of the initial development of zinc electrodeposits grown with the forced fluid flow applied quasi-parallel to the imposed electric field. The growth area directly exposed to the fluid flow corresponds to the south hemisphere of the presented images. Conditions are as in Fig. 1 for (a) 0 rpm and (b) 12 rpm.

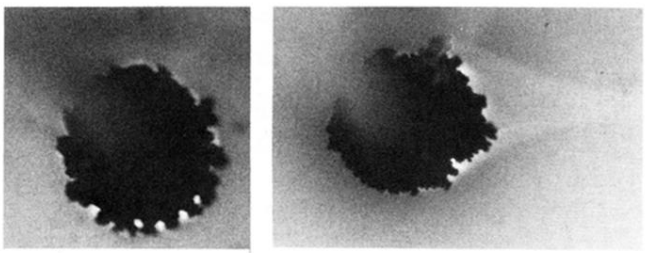

(a) (b)

FIG. 6. Images of electrodeposition of copper evidencing the concentration boundary layer. Flow conditions are (a) 0 rpm and (b) 3 rpm. The size of the deposits is about 1 mm.